

Meso Mechanical Analysis of AC Mixture Response

Milliyon Woldekidan ¹, Marinus Huurman ², Elisa Vaccari ³, Marco Poot ⁴

(1 Delft University of Technology, Stevinweg 1, 2600 GA Delft, The Netherlands,
m.f.woldekidan@tudelft.nl)

(2 Delft University of Technology, Stevinweg 1, 2600 GA Delft, The Netherlands,
m.huurman@tudelft.nl)

(3 Delft University of Technology, Stevinweg 1, 2600 GA Delft, The Netherlands,
e.vaccari@tudelft.nl)

(4 Delft University of Technology, Stevinweg 1, 2600 GA Delft, The Netherlands,
m.r.poot@tudelft.nl)

ABSTRACT

Ongoing research into performance modeling of Asphalt Concrete (AC) mixtures using meso mechanics approaches is being undertaken at Delft University of Technology (TUD). The approach has already been successfully employed for evaluating the long term performance of porous asphalt concrete. The work presented in this paper extends the use for predicting the uni-axial response of AC mixtures. The approach demands the meso-scale geometry, the loading and the mechanical behavior of the component materials for the AC mixture to be specified. For this purpose, laboratory tests were first carried out on a bituminous mortar. Then, rectangular AC mixture specimens were prepared in the laboratory. The four sides of the AC specimens were scanned to capture the two dimensional (2D) meso-scale geometry of the mixture. The scanned images were then processed and translated into meso-scale finite element models. Viscoelastic model parameters for the mortar were determined from experimental data. The FE models were then used to simulate the frequency domain response of the AC mixture in a uni-axial mode. Similarly, uni-axial tests were carried out in the laboratory to obtain the frequency domain response of the AC mixture. FE simulated and experimental results were then compared. Good agreements in results have been obtained. The paper thoroughly discusses the obtained results and its implications for developing mixture design tools.

Keywords: meso-mechanics, viscoelastic, master curve, asphalt mixture, mortar .

1 INTRODUCTION

Predicting the mechanical behavior of heterogeneous materials, such as asphalt concrete mixtures, is highly complex. This is because the mechanical behavior of a composite material is highly influenced by the intricately complex interaction of the various component materials. The component materials in a typical AC mixture include air voids, bituminous mortars and aggregate particles. Further more, the bituminous mortar is composed of fillers and sands. Under a mechanical loading; the component material's mechanical behavior, spatial distribution, meso structure and their interaction highly influences the bulk mixture behavior, which in turn is related to performance characteristics such as fatigue and rutting resistance. Mechanistic design tools that take into account the effects of the component materials behavior, meso scale geometry and loading are highly sought for to provide valuable insight into the in-mixture phenomenon to ultimately understand mixture performance characteristics.

For gaining insight into the performance characteristics of heterogeneous materials like AC mixtures, meso-mechanics approaches are best suited. This is due to their intrinsic nature that allows prediction of bulk mixture response by taking into account the meso scale geometry and the behavior of component materials. Because of such merits, the approach has increasingly been used for predicting AC mixture response [1-3]. For performance modeling of thin surface seals, the

approach was first employed in the early 2000 [4]. Recently, the approach has further been utilized to develop a design tool for porous asphalt concrete layers [5-7].

In meso-mechanics two modeling approaches are commonly used, i.e. continuum Finite Element Method (FEM) and Discrete Element Method (DEM). Continuum FEM models are efficient in evaluating stresses and strains in a continuum media such as bituminous mortar in AC mixtures. This modeling approach is also computationally efficient as compared to DEM approach. On the other hand, DEM models are best suited to model systems involving large deformations and discontinuities. DEM works with defined contact laws between particles, and it is proven to be suitable for modeling granulate matters. The approach, however, requires huge computational power as compared to the FEM approach.

In this paper, FEM based meso mechanical model is utilized to predict the mechanical behavior of AC mixture. First, a slightly over filled stone mastic asphalt mixtures were prepared in the laboratory. The slightly higher bitumen content is meant to minimize stone-stone contact phenomenon in the AC meso structure. The AC mixtures were made with gyratory compactor. From the prepared AC mixtures, rectangular test specimens were cut for uni-axial testing. Then, the meso-scale geometry of the AC specimens was obtained through image scanning. The scanned images were then transformed into FEM models to allow computer simulation of laboratory tests. In the modeling approach aggregate particles were considered as rigid bodies, and the mortar behavior was assigned viscoelastic behavior. The viscoelastic parameters of the bituminous mortar were determined from test results that were obtained from Dynamic Shear Rheometer (DSR) tests. The meso mechanical FEM models were then finally used to simulate uni-axial tests at various frequencies. The applied displacement and simulated load signals were analyzed to predict the mechanical behaviour of the AC mixture.

In the laboratory, the frequency domain response of the AC mixture was also investigated at various frequencies and temperatures. Results obtained from the laboratory tests are compared with the simulation results. Good agreement in results is obtained. The results have further demonstrated the capability of the meso mechanics in predicting AC mixture response. The paper presents the details of the experimental and modeling work, and outlines pressing modeling issues that need to be addressed in the future.

2 EXPERIMENTAL WORK

The experimental work carried out in this work comprises of AC mixture and mortar testing. For mortar testing, a DSR test setup with relevant mortar column geometry was used. For the AC mixture testing, a Universal Testing Machine (UTM) was utilized. Details on the composition of the materials and description of the test setups are given in the following sections.

2.1 DSR Testing of Mortar

The bituminous mortar used in this research composed of 70-100 penetration grade bitumen, Wigro 60K lime stone filler, with 25% chalk hydrate, and fine fractions of sand with maximum particle size of 0.5 mm. Due to the presence of sand particles in the mortar, a specially designed specimen geometry is utilized (see Fig.1). This setup was originally developed during previous meso-mechanics project for PA mixtures [5, 8-11]. The mortar specimen has a total height of 20 mm and a central diameter of 6 mm. At the two ends, it is equipped with steel rings to allow clamping of the mortar specimen onto the DSR machine.

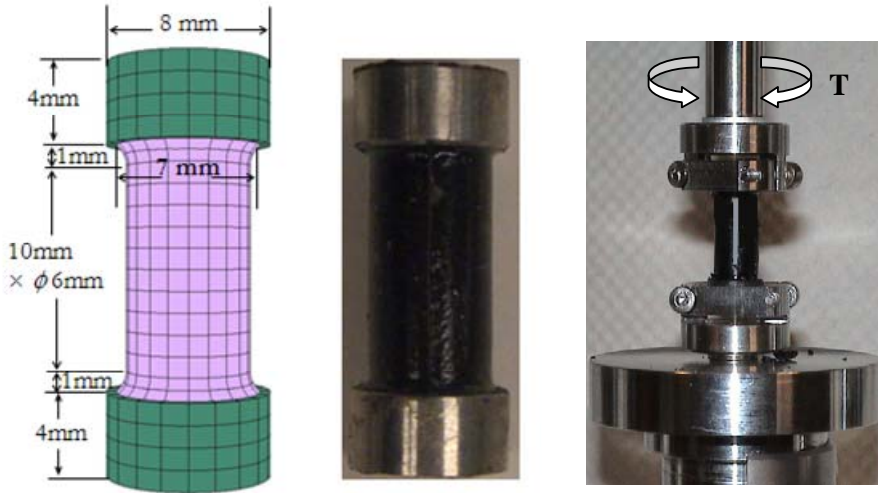


Fig.1 Mortar specimen (left: FE model, Middle; mortar specimen, Right; mounted specimen)

Using the test setup shown in Fig.1, DSR frequency sweep tests were carried out on the mortar for temperatures varying from -10°C to 30°C . The obtained results were then used to construct a master curve at a selected reference temperature. Such master curve provides the necessary viscoelastic model parameters of the mortar for FE simulations.

2.2 Uni-Axial Tests on AC mixture

The AC mixture used in this work is a Stone Mastic Asphalt (SMA) mix. According to the Dutch specification [12], the required amount of materials was first determined. A slightly over-filled mixture was selected to minimize the occurrence of stone-stone contact phenomenon. The composition of the selected mixture is given in Table 1.

Table 1. SMA mixture composition

Size (mm)	Dutch Spec. % retained	% retained cumulative	Mass (gram)
11.2-8	0-8	0	0
8-5.6	45-65	45	1085.69
5.6-2	70-80	80	844.43
2-0.63	89-93	93	313.60
Filler <0.63	100	100	168.6
Bitumen	7.5	108	193.0

In the mixture preparation stage, 150 mm diameter AC samples were produced using a gyratory compactor. From the gyratory samples, rectangular test specimens with dimensions of 40 mm x 40 mm x 100 mm were cut. Out of four test specimens, the best two samples were selected based on visual inspection. Fig.2 shows the four different rectangular test specimens out of which the best two samples are selected. In reference to Fig.2, specimen 1 and specimen 4 were discarded due to the presence of high voids on the surfaces of the specimens. For the modeling work presented in this paper specimen 3 was utilized.



Fig. 2 AC mixture specimens

The two ends of the selected specimens were then polished. Aluminum end-caps were also prepared to allow mounting of the test specimens to the UTM machine. The mounting procedure involves gluing one end of the specimen to the Aluminum end-cap using two-component fast curing adhesive glue (X60). The glued-end is then mounted to the UTM machine before the other end of the specimen is glued (see Fig.3). For measuring deformations, three strain transducers (LVDT) were mounted on the specimen. For testing, the specimen is then conditioned at the test temperature for about two hours. Then force controlled, uni-axial dynamic tests were conducted for frequencies ranging from 1 Hz to 10 Hz at various temperatures. The resulting deformation signals were then analyzed to obtain the dynamic modulus and phase angle properties of the AC specimens.



Fig.3 Uni-axial setup: mounting procedures (left and middle), strain transducers (right)

4 TIME TEMPERATURE SUPERPOSITION PRINCIPLE

From mechanical tests performed at various temperatures, the response data of a bituminous material can be brought together to form a master curve at a selected reference temperature by using time-temperature superposition principle. The shift factor required at the various temperatures to form the master curve indicates the temperature susceptibility of a material. It is usually described by using the Arrhenius or the Williams-Landel-Ferry (WLF) equation [13]. For both the asphalt mixture and the mortar data, the WLF relation given in Eq.(1) has been used.

$$\text{Log } a_T = \frac{-C_1(T - T_0)}{C_2 + (T - T_0)} \quad (1)$$

Where C_1 and C_2 are constants; T is the temperature in °C; T_0 is the reference temperature in °C and a_T is the shift factor. To allow automatic determination of shift factor parameters in regression analysis, a master curve model was utilized. For bituminous materials, various master curve models are available in literature [14-16]. In this work, the modified HS (MHS) model has been used to describe the master curve. This model is obtained by placing a linear dashpot in series with the original Huet-Sayegh model. The MHS model for describing the frequency domain response data of a viscoelastic material is given as [16]:

$$(G^*(\omega))^{-1} = \left(G_0 + \frac{G_\infty - G_0}{1 + \delta(i\omega\tau)^{-m_1} + (i\omega\tau)^{-m_2}} \right)^{-1} - \frac{i}{\eta_3\omega} \quad (2)$$

Where $G^*(\omega)$ denote the complex modulus; G_0 , G_∞ , δ , τ , m_1 , m_2 and η_3 are model parameters, and i denotes imaginary number in complex number notation. If the G_0 value is nil, the model reduces to the familiar 2S2P1D model.

5 AC MESO MECHANICAL MODELING

The FEM modeling is performed using a commercially available FE program, ABAQUS. Based on the images taken from the four sides of the AC specimen, the meso-scale geometry is captured as a two dimensional model. In the modeling approach a plane-strain assumption has been used. With regard to the mechanical properties of the component materials, aggregate particles were treated as rigid bodies. This is on the assumption that the deformation contribution from the individual aggregate particles are not of major significance as compared to the deformation contribution from the bituminous mortar. The bituminous mortar is modeled as viscoelastic material. In the following section, details on modeling approach are further discussed.

5.1 Modeling the Meso-Scale Geometry

To model the meso-scale geometry of the AC specimens, images that were taken from the four sides of the AC specimen were utilized. For the work presented in this article, specimen no 3 has been selected. To allow a clear distinction between air voids and mortar on the 2D images, the air voids on the specimen surface were first filled with a white substance (chalk) before images were taken. Then FEM models were then developed based on the 2D images. In the modeling process, identification of the individual aggregate particles and air voids is performed manually. Fig.4 illustrates the transformation process: the original image is first set as a backdrop in a FE program and the aggregate particles are traced as a partition. Air voids are created by cutting through the mortar part. Since the aim is to predict the mechanical behavior of the bulk AC mixture, adhesive layer to represent stone-mortar interface has not been provided in this model. However, for PA performance models in previous works, such provisions have been made. For detailed information on FE model transformation and adhesive layer modeling, the reader is referred to previous meso mechanical modeling works [7, 17]. In the FE model given in Fig.4, the end-caps that were used at the two ends of the specimen are also included. Similar models were prepared for the remaining three faces of the AC specimen. The FE models were then meshed using an eight node quadratic element. To evaluate the effects of 2D generalizations, i.e., plane strain versus plane stress assumption, the authors are undertaking further study based on 3D modeling. This, however, has not been covered in this article. The results presented in this work are based on a plane strain assumption.

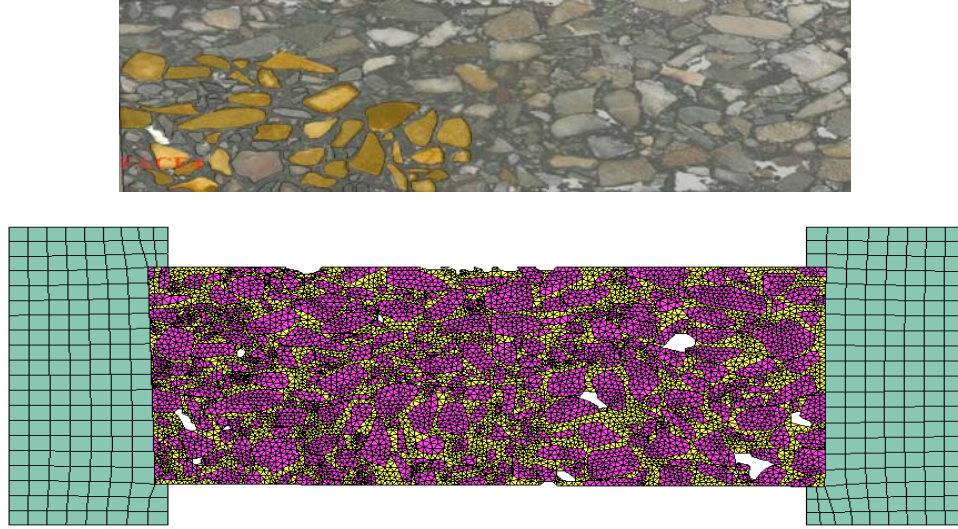


Fig.4 Image used as a back drop in FE model development (top), and the completed FE model with Aluminum end-caps (bottom)

5.2 Component Material Behavior

To allow prediction of the bulk mechanical behavior, the mechanical properties of the component materials need to be known. The utilized approach assigns elastic property for the Aluminum end-caps, viscoelastic property for the mortar and rigid body for the stone particles. The most widely used rheological models in FE environments include the Prony series and Burgers' model. Recently, for models comprising of parabolic dashpots, such as the Huet-Sayegh, 2S2P1D and MHS, method of numerical implementation using a fractional approach has been illustrated [16]. While models comprising of linear spring and dashpot are generally efficient in numerical environments, models comprising parabolic dashpot are efficient in accurately describing material response with few model parameters. In terms of results in numerical environments, both categories of models appear to provide comparable results provided the utilized model parameters describe the experimental response data with comparable accuracy. In this work, for reasons of numerical efficiency, the Prony series model given in Eq.(3) is utilized

$$G(t) = G_r + \sum_{i=1}^n G_i \cdot e^{-t/\tau_i} \quad (3)$$

In Eq.(3), the parameters G_r , G_i and τ_i denote the rubbery shear modulus, relaxation strength and relaxation times respectively. The corresponding expression for describing frequency domain experimental data is given as;

$$G'(\omega) = G_r + \sum_{i=1}^n \frac{G_i \tau_i^2 \omega^2}{1 + \tau_i^2 \omega^2}; \quad G''(\omega) = \sum_{i=1}^n \frac{G_i \tau_i \omega}{1 + \tau_i^2 \omega^2} \quad (4)$$

Where $G'(\omega)$, $G''(\omega)$ represent the storage shear modulus and loss shear modulus, respectively. For determination of Prony model parameters the relation given in Eq.(4) was fitted to a mortar master curve data. The collocation method proposed by Schapery has been utilized [18].

6 RESULTS

6.1 Mortar Master Curve

Results obtained from frequency sweep tests for temperatures in the range of -10°C to 30°C were used to construct a master curve for the mortar. The data comprises results obtained from tests conducted on 5 different mortar specimens. The master curve obtained at a reference temperature of 10°C is shown in Fig.5. The WLF shift factors and the MHS model parameters corresponding to the master curve are given in Table 2.

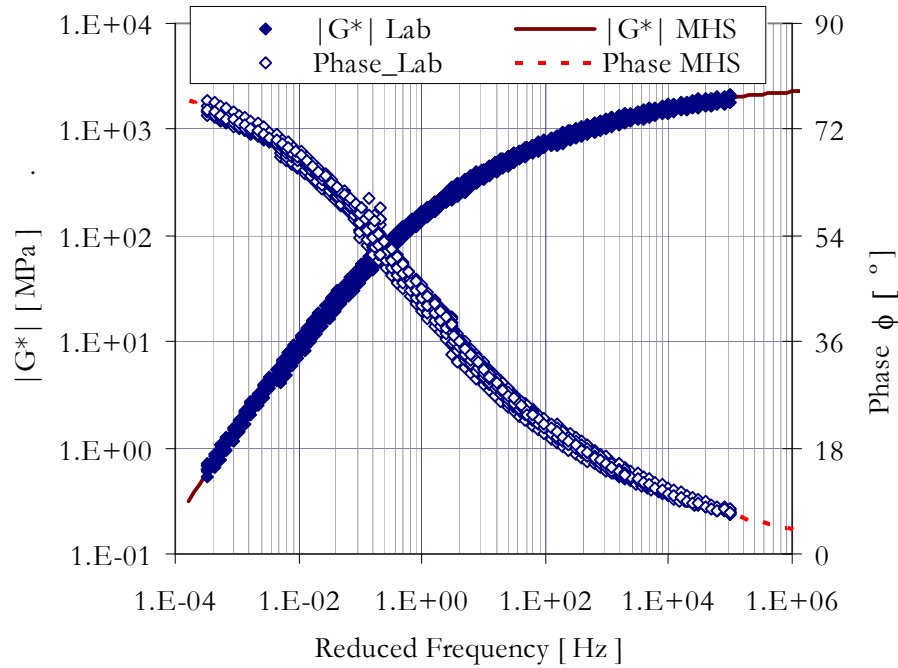


Fig.5 Mortar master curve at a reference temperature of 10°C

Table 2. WLF factors and MHS model parameters for mortar at $T_{\text{ref}}=10^{\circ}\text{C}$

WLF Factors		MHS model parameters						
C_1	C_2	m_1	m_2	δ_1	τ	G_{∞}	G_0	η_3
(-)	(-)	(-)	(-)	(-)	(s)	(MPa)	(MPa)	(MPa.s)
21.88	160.9	0.711	0.272	2.87E-2	5.41E-5	2474	0	585.44

Table 3. Prony series model parameters for mortar (12 terms), $T_{\text{ref}}=10^{\circ}\text{C}$

G_0 (MPa)	1749.2						
τ_i (s)	4.12E-5	1.7E-4	7.0E-4	2.9E-3	1.2E-2	4.9E-2	
α_i (-)	3.66E-1	5.0E-2	2.13E-1	1.07E-1	1.1E-1	7.3E-2	
τ_i (s)	2.0E-1	8.4E-1	3.5	14.3	58.8	242.4	
α_i (-)	4.9E-2	2.1E-2	6.3E-3	2.0E-3	4E-4	2.2E-4	

Corresponding to the MHS model parameters given in Table 2, equivalent Prony series model parameters were also determined for use in numerical model. The 12-term Prony series model parameters determined at a reference temperature of 10°C are presented in Table 3.

6.2 AC Mixture Master Curve

Following the same approaches as used for the mortar, the uni-axial experimental data obtained at various temperatures for the AC mixture was used to construct a master curve. Due to limitations to perform tests for wide range of frequencies in the UTM machine, measurements were conducted at three distinct frequencies, i.e. 1 Hz, 5 Hz and 10 Hz at each temperature. For these frequencies, temperatures ranges varying from -10°C to 30°C were covered. The applied load and measured deformation signals were analyzed to determine the dynamic modulus and phase angle data of the AC mixture. With these data a master curve was constructed at a reference temperature of 10°C. Fig.6 presents the experimental and master curve data for the mixture. The corresponding WLF shift factor and MHS model parameters are given in Table 4.

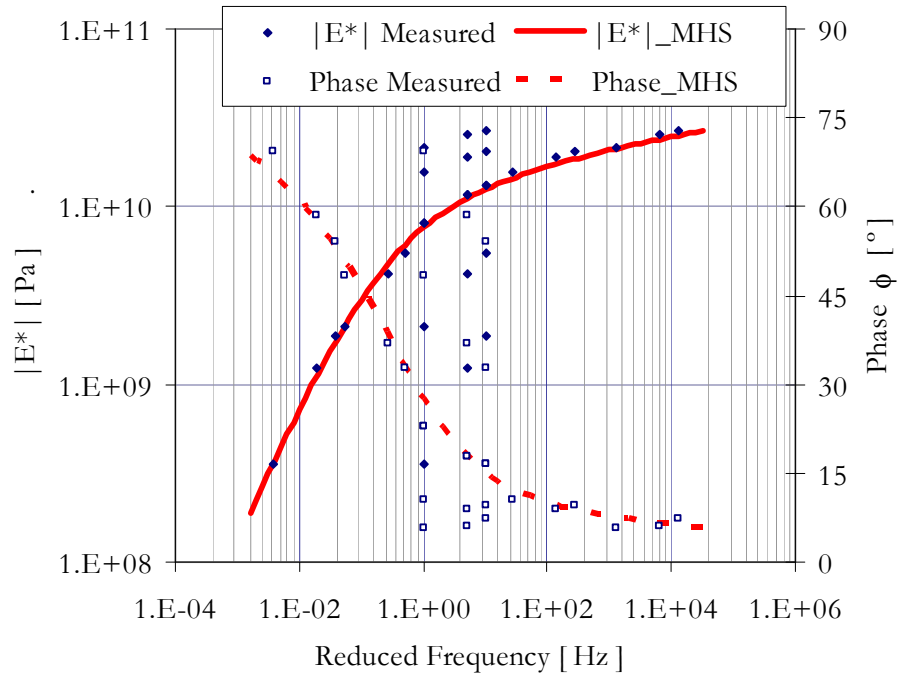


Fig.6 AC mixture master curve at a reference temperature of 10°C

Table 4. WLF factors and MHS model parameters for AC mixture, $T_{ref}=10^0C$

WLF Factors		MHS model parameters						
C_1	C_2	m_1	m_2	δ_1	τ	E_∞	E_0	λ_3
(-)	(-)	(-)	(-)	(-)	(s)	(MPa)	(MPa)	(MPa.s)
21.88	160.9	0.144	0.659	2.80	4.62E-2	4.65E4	0	5.0E4

In Table 4, the notations for the MHS model parameters; E_∞ , E_0 and λ_3 are used to indicate the properties correspond to the uni-axial rather than the shear properties of the AC mixture. Similar to the mortar master curve presented in Fig.5, the AC mixture master curve in Fig.6 is also well described by the MHS model. In constructing the master curve it was observed that the temperature susceptibility of the AC mixture remains the same as the mortar. This can be seen from the similar WLF factors used for mortar and AC master curves (Table 2 and Table 4).

6.3 Meso-Mechanical FEM Simulations

Displacement controlled uni-axial tests were simulated using the FEM models at various frequencies and temperatures. At each temperature, sinusoidal displacements with frequencies of 0.1, 1, 5, 10 and 100 Hz, were applied, and the simulated load signals were analyzed. In the

simulation the mortar behavior at a reference temperature of 10°C, Table 3, was used. Relevant Prony series parameters for simulations at other temperatures were determined by using TTS principle. For this purpose, the WLF parameters in Table 2 were utilized. For the Aluminum end-caps an elastic property with $E=2G$ Pa and Poisson's ratio of 0.2 was used. Impressions of the two dimensional FE models for the four faces of the AC specimen are given in Fig.7. The models illustrate the distinct aggregate particles, the mortar component and air voids in the mixture.

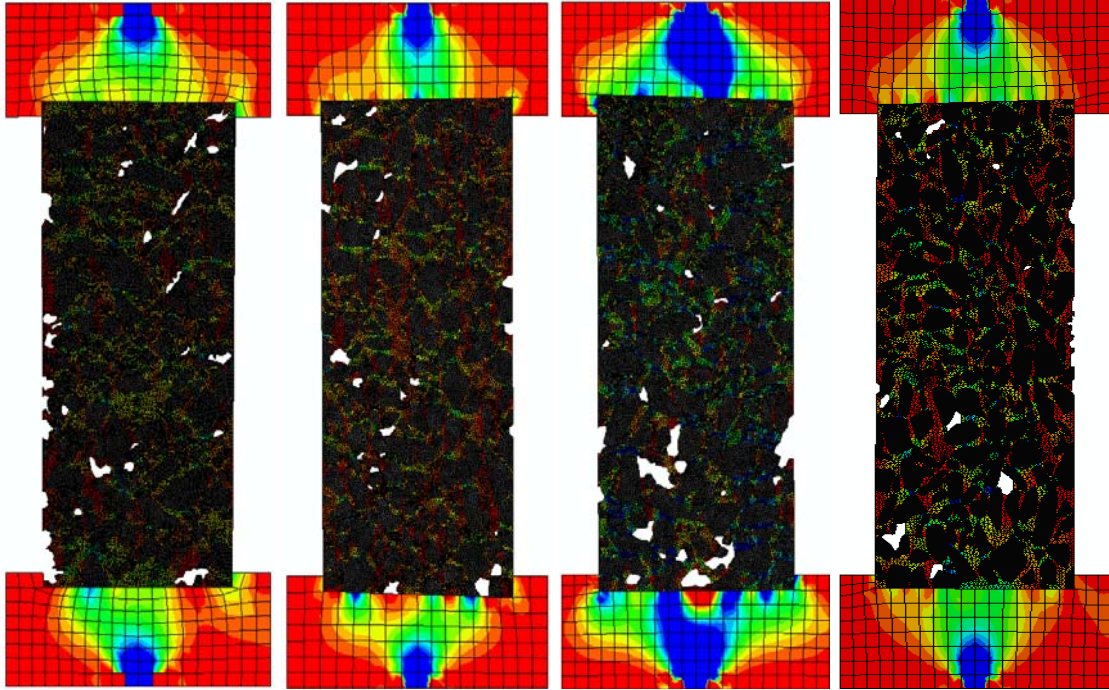


Fig.7 2D FE models developed from the 4 faces of the AC specimen

In determining the complex modulus and phase angle data, signals of 10 to 15 cycles were analyzed at each frequency. The resulting data for the complex modulus and phase angle were then used to construct a master curve at a reference temperature of 10°C utilizing the shift factors given in Table 2. Alternatively, same master curve results can be simulated by performing the FE computations at a reference temperature of 10°C at various reduced frequencies. Simulated master curve results obtained from the four FE models are presented in Fig.8. It can be seen from Fig.8 that the simulated complex modulus and Phase angle data from the four faces of the specimen show some scatter. This scatter can be attributed to the difference in meso-scale geometry of the four faces of the specimen (see Fig.7). To obtain a representative curve for the simulated results, a master curve equation has been fitted to the simulated data. The FE simulated data from the four models and the fitted master curve are shown in Fig.8.

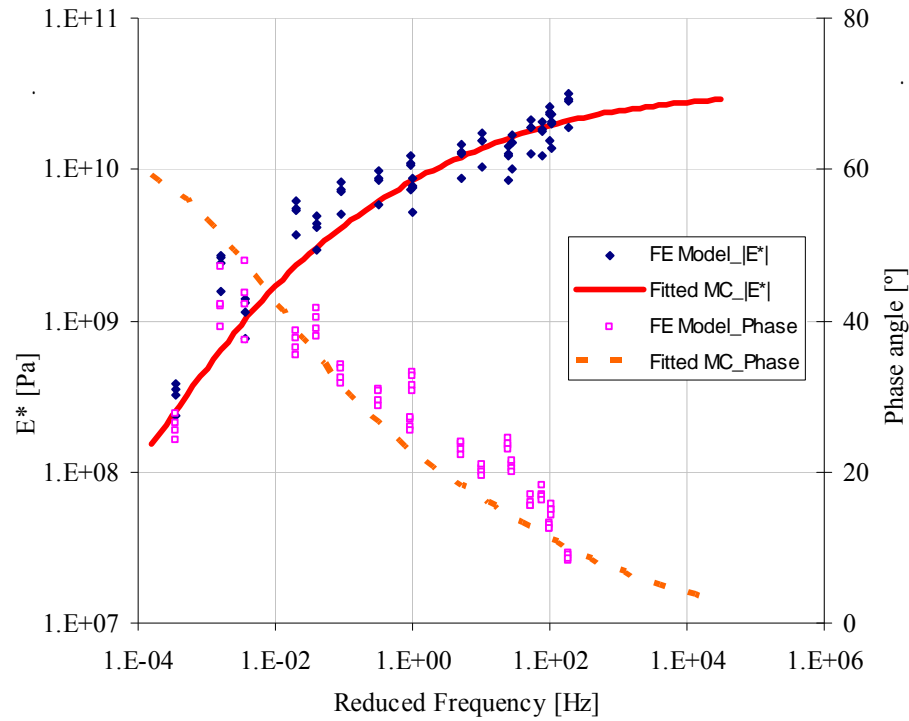


Fig. 8 FE simulated data and fitted master curve for the AC specimen, $T_{ref} = 10^{\circ}\text{C}$

For comparison, the fitted master curve from Fig.8 is presented together with the master curve presented in Fig.6, which was obtained from the laboratory data. The comparison is presented in Fig.9. The comparison shows that the meso-mechanics predictions are in good agreement with the laboratory data especially at lower temperature regions. At higher temperatures, the FE model predictions overestimated the complex modulus data.

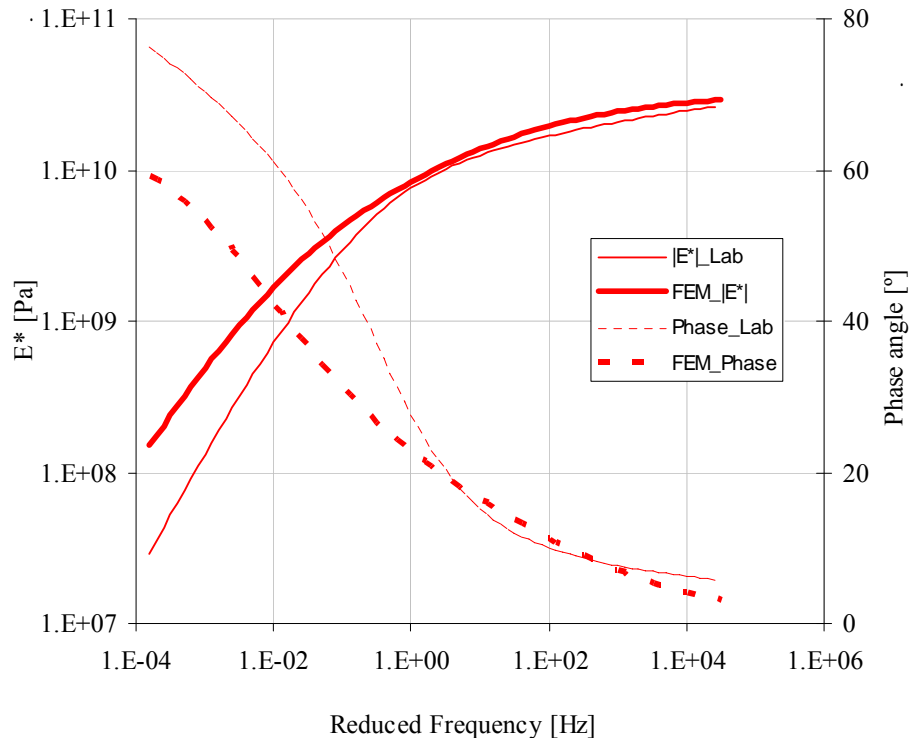


Fig.9 Master Curve comparison: experimental and FEM prediction at 10°C

From Fig.9, it can be seen that the meso mechanical model predictions are in good agreement at higher frequency regions, which correspond to the lower temperature data. The distinct discrepancy at higher temperatures or lower frequency region can be attributed to many factors. One possible factor could be in relation to geometrical nonlinearity. At lower temperature, where the bitumen material is relatively stiffer, effects resulting from deformation-related nonlinearity on the measured and simulated results are less than those at higher temperatures. In order to take into account the geometrical nonlinear effects both in the simulation and laboratory work, the laboratory tests need to be carried out for similar loading condition as used in the simulation. However, due to the UTM machine limitation the experimental work was carried out in force controlled while the simulation was performed in strain controlled manner. Further investigation on this can be made in the future by performing force controlled FE simulations for similar loading conditions as used in the laboratory. Other factor that needs to be considered is the possibility of aggregate-aggregate interaction at higher temperatures which was not considered in the modeling approach utilized in this paper. Further investigations on these as well as other possible effects, such as plane-strain versus plane-stress approaches on the simulation results, are to be performed in future works. Performing similar simulations with discrete element modeling for higher temperature could also provide additional insight on the effects of large deformations on measured results.

7 CONCLUSIONS

This paper presented a FEM approach for modeling the response behavior of AC mixtures. The meso-scale geometry of the AC mixture was captured using images obtained from the four faces of the AC specimen. The images were translated into two dimensional FE models. The obtained meso-mechanical FE models depict the different components of the AC mixture, namely the stone aggregates, the bituminous mortar and air voids. Relevant mechanical properties were assigned to the component materials, and frequency domain tests were simulated using the FEM models. Similarly, experimental measurement was carried out on the AC mixture to obtain the response of the mixture at various frequencies and temperatures. The FE simulated and experimentally obtained mixture responses were compared. The results have shown good agreement at lower temperature regions. At higher temperatures, the FE simulated response overestimated the actual mixture response. The results in general have shown the remarkable potential of meso-mechanics approach in predicting AC mixture response. For future meso mechanical analysis of mixtures at high temperatures, where large deformations are likely to occur, modeling with discrete element or hybrid (FEM-DEM) models may also be employed. With the availability of these numerical modeling techniques, meso mechanics approach can further be utilized for developing mechanistic mixture design tools that allow mixture performance evaluations such as rutting and cracking.

REFERENCES

- [1]. Buttlar, W. and Z. You, *Discrete Element Modeling of Asphalt Concrete: Microfabric Approach*. Transportation Research Record: Journal of the Transportation Research Board, 2001. **1757**(-1): p. 111-118.
- [2]. Dai, Q., M.H. Sadd, and Z. You, *A micro-mechanical finite element model for visco-elastic creep and visco-elastic damage behavior of asphalt mixture*. Int J Numeric Anal Meth Geomech, 2006. **30**: p. 1135-1158.
- [3]. Papagiannakis, A., A. Abbas, and E. Masad, *Micromechanical Analysis of Viscoelastic Properties of Asphalt Concretes*. Transportation Research Record: Journal of the Transportation Research Board, 2002. **1789**(-1): p. 113-120.
- [4]. Huurman, M., T.I. Milne, and M.F.C. Van de Ven, *Development of a structural FEM for road surfacing seals*, in *ICCES*. 2003: Corfu, Greece.
- [5]. Huurman, M., L. Mo, and M. Woldekidan, *Mechanistic Design of Silent Asphalt Mixtures*. International Journal of Pavement Research and Technology, 2010. **3**(2): p. 56-64.

- [6]. Huurman, M., L. Mo, and M.F. Woldekidan, *Unravelling Porous Asphalt Concrete, Towards a Mechanistic Material Design Tool*. Int. Journal Road Materials and Pavement Design, 2009. **10**(Special Issue).
- [7]. Huurman, M., et al., *Overview of the LOT meso mechanical research into porous asphalt raveling*. Advanced Testing and Characterisation of Bituminous Materials, Vols 1 and 2, 2009: p. 507-518.
- [8]. Huurman, M., L.T. Mo, and M.F. Woldekidan, *Unravelling Porous Asphalt Concrete, Towards a Mechanistic Material Design Tool*. Road Materials and Pavement Design, 2009. **10**: p. 233-262.
- [9]. Mo, L.T., et al., *Investigation into material optimization and development for improved ravelling resistant porous asphalt concrete*. Materials & Design, 2010. **31**(7): p. 3194-3206.
- [10]. Woldekidan, M., M. Huurman, and L. Mo, *Testing and modeling of bituminous mortar response*. Journal of Wuhan University of Technology--Materials Science Edition, 2010. **25**(4): p. 637-640.
- [11]. Woldekidan, M.F., M. Huurman, and A.C. Pronk. *Towards an accurate stress dependent time & frequency domain ve response model for bituminous binders*. in *The 11th international conference on asphalt pavements*. 2010. Nagoya, Japan.
- [12]. RAW, *Standaard RAW Bepalingen 2005*. 2005: Ede.
- [13]. Ferry, J.D., *Viscoelastic properties of Polymers*. 3rd edition ed. 1980, New York.
- [14]. Pronk, A.C. *The Huet-Sayegh Model: A Simple and Excellent Rheological Model for Master Curves of Asphaltic Mixes*. 2005. Baton Rouge, Louisiana, USA: ASCE.
- [15]. Benedetto, H.D., et al., *Three-dimensional Thermo-viscoplastic Behaviour of Bituminous Materials. The DBN Model*. Road Materials and Pavement Design, 2007. **8**(2): p. 285-315.
- [16]. Woldekidan, M.F., M. Huurman, and A.C. Pronk, *A modified HS model: Numerical applications in modeling the response of bituminous materials*. Finite Elements in Analysis and Design, 2012. **53**(0): p. 37-47.
- [17]. Huurman, M., *Lifetime Optimisation Tool, LOT, Main Report*. 2008: Delft.
- [18]. Schapery, R.A., *A simple Collocation Method for Fitting Viscoelastic Models to Experimental Data*. 1961, California Institute of Technology: Pasadena, California.